

## 2.5 Additional Heating and Current Drive

2.5.1	Neutral Beam Injection System	2
2.5.1.1	System Parameters	2
2.5.1.2	System Layout and Integration	3
2.5.1.3	System Design	3
2.5.1.4	Component Design	6
2.5.1.5	Diagnostic Neutral Beam	10
2.5.1.6	Maintenance	11
2.5.1.7	Design Assessment	11
2.5.2	Radio-Frequency Systems	1
2.5.2.1	General Design Features of the RF Heating and Current Drive Systems	12
2.5.2.2	Layout	12
2.5.2.3	Electro-mechanical Analysis	15
2.5.2.4	Commissioning and Operation	17
2.5.2.5	Maintenance	18
2.5.2.6	Design Assessment	19
2.5.3	Electron Cyclotron System	20
2.5.3.1	General Design Features	20
2.5.3.2	Launcher(s) Design	21
2.5.3.3	Power Transmission Design	24
2.5.3.4	Power Source	25
2.5.4	Ion Cyclotron H&CD System	25
2.5.4.1	General Design Features	25
2.5.4.2	Launcher Design	27
2.5.4.3	Power Transmission Design	29
2.5.4.4	RF Power Sources	29
2.5.5	Lower Hybrid System	29
2.5.5.1	General Design Features	29
2.5.5.2	Launcher Design	30
2.5.5.3	Power Transmission Design	31
2.5.5.4	RF Power Sources	33

Multiple roles and a wide range of functions are assigned to the additional heating and current drive (H&CD) systems in ITER.

All key phases of the reference scenario – i) the access to the H-mode regime, ii) the plasma temperature rise, while density is increased to allow the requisite fusion power, iii) the achievement of a steady burn, iv) the control of the excursions about the operating point, v) the suppression of instabilities, and vi) the achievement of a soft termination – are controlled by the input of H&CD power by an appropriate combination of neutral beams (NBs) and three RF H&CD systems operating at the electron cyclotron (EC), ion cyclotron (IC) and lower hybrid (LH) frequency. The last will not be used for initial operation and may be added only in an upgrade of H&CD performance.

The onset of neo-classical tearing modes (NTMs) potentially poses challenges to ITER high-operation and provisions for active control by ECCD is included.

H&CD systems are required to heat non-fusion plasmas in the early operating phases, for example, to commission the divertor target plates. They are used for plasma initiation and assisted start-up, to control sawteeth and resistive wall modes, to induce a small amount of plasma rotation, and for wall conditioning.

Steady state operation requires an on-axis current seed and active control of the plasma current profile, to access enhanced confinement regimes in which a large fraction of the plasma current is generated via the bootstrap effect.

With the current number and dimensions of the ITER ports competition for access to the plasma is tight. For H&CD systems, this is reflected in the need for high power density operation, close to the practical limit.

Two and possibly three ports are reserved for the NB injectors, two equatorial ports are assigned to RF systems, and three additional upper ports are used for ECCD NTMs stabilisation. For the equatorial ports, the design power density is 20 MW/port for the RF systems and 16.5 MW/port for the NB H&CD system. Seven MW of EC power can be injected in each upper port.

Provision is made in the design for space, auxiliaries and services adequate for the maximum installed power, i.e. for four equatorial ports (and three upper ports) for RF power and 3 NB injectors. With all auxiliary systems operating at the nominal performance in all possible reserved ports, 130 MW of H&CD power would be available, although heating power of only up to 110 MW should be added simultaneously to the plasma.

## **2.5.1 Neutral Beam Injection System**

### **2.5.1.1 System Parameters**

The neutral beam (NB) system design consists at present of two heating and current drive (H&CD) injectors and one diagnostic neutral beam (DNB) injector (2.5.1.5). Each H&CD injector will deliver a deuterium beam of 16.5 MW (total 33 MW), with energy of 1 MeV, and will be able to operate for long pulses (up to 3,600 s for steady state operation). A system based on negative ( $D^-$ ) ions is necessary, primarily, for better energy efficiency due to its high neutralisation efficiency.

The size of the ion source and the required  $D^-$  current density should not require large extrapolations from the largest operational negative-ion-based NB injection systems (JT-60U and LHD N-NB injection systems) in physics (plasma uniformity and negative ion current density) and in engineering (manufacturing, assembly, and maintenance) aspects. The present design assumes 200 A/m<sup>2</sup> as the  $D^-$  accelerated current density, at the grounded grid (a reasonable extrapolation from the relevant R&D results), a total accelerated current of 40 A and an ion source roughly twice the size of that on the JT-60U N-NB injection system.

The acceleration voltage remains the only free variable. For the H&CD injectors, higher voltages than the one quoted above could permit to increase the power and the current drive efficiency. On the other hand, higher voltages imply larger insulation distances (both in gas and vacuum) and higher beam shine-through through the plasma. Moreover, the maximum acceleration voltage of the two existing test beds, at Naka and at Cadarache, is 1MV in both cases. Considering ITER dimensions, 1 MV is considered as a good compromise.

In addition to heating and current drive, a small amount of plasma rotation is also provided by the NB H&CD injectors. For the H operation phase, the H&CD injectors can be operated in hydrogen, with beam energy 0.8 MeV and beam power 13 MW.

### 2.5.1.2 System Layout and Integration

Figure 2.5.1-1 shows the NB layout: the NB injectors are located on the north side, at the equatorial level of the tokamak building. Port 4 is shared between an H&CD injector and the diagnostic injector, and port 5 is allocated to the second H&CD injector. Space has been reserved for a third injector that could be mounted on port 6. The total NB H&CD power could then reach 50 MW

The horizontal angle of injection is defined by the NB duct size (including beam envelope, vacuum confinement, neutron shielding, tolerances and clearances) and the space available between the toroidal field coils (see Figure 2.5.1-2). The strike area on the far wall of the vacuum vessel is constrained not to include a port so as not to damage items in the port plug. Beam injection is possible when the plasma density is  $0.35 \times 10^{20} \text{ m}^{-3}$ , assuming that  $1 \text{ MW/m}^2$  is the acceptable power density on the first wall.

Within the NB duct height, the beam can be aimed at two extreme (on-axis and off-axis) positions by tilting the beam source around a horizontal axis on its support flange. In order to cover a range of vertical positions from the machine equatorial plane (at the tangency point) suitable for both on- and off-axis CD, the beam axis is tilted vertically in the range 40 - 60 mrad. This tilted beam geometry enables the NB duct to be compatible with a port of the same height as the regular equatorial port, the other relevant structures of the machine (toroidal field coils, intercoil structures, poloidal field coils and thermal shields) and the building design. The main layout parameters are listed in Table 2.5.1-1.

**Table 2.5.1-1 System Layout, Main Parameters**

Beam Tangency Radius (mm)	Beam Axis Vertical Position from the Equatorial Plane, at Tangency Radius (mm)		Duct Liner Exit Width (mm)	Duct Liner Exit Height (mm)	Distance from Grounded Grid to Duct Liner Exit (m)
	Highest	Lowest			
5300 ± 60	+ 156	- 417	582	1360	22.8

The injector's vessel is an extension of the primary vacuum boundary and is part of the primary barrier for contamination confinement. The common enclosure for all the injectors, the NB cell, performs the function of a secondary confinement barrier.

### 2.5.1.3 System Design

Figure 2.5.1-3 shows the NB system design. Since the early stages of the EDA, the injector has been conceived with the aim to reduce its axial length, and hence to limit the cost impact on the tokamak building. The concept<sup>1</sup> is to subdivide the neutralizer, and, consequently, the residual ion dump (RID) to form four vertical channels.

<sup>1</sup> R Hemsworth, et al., "Neutral Beams for ITER", Rev. Sci. Instrum. 67/3 Part II, pp 1120 - 1125, (1996).



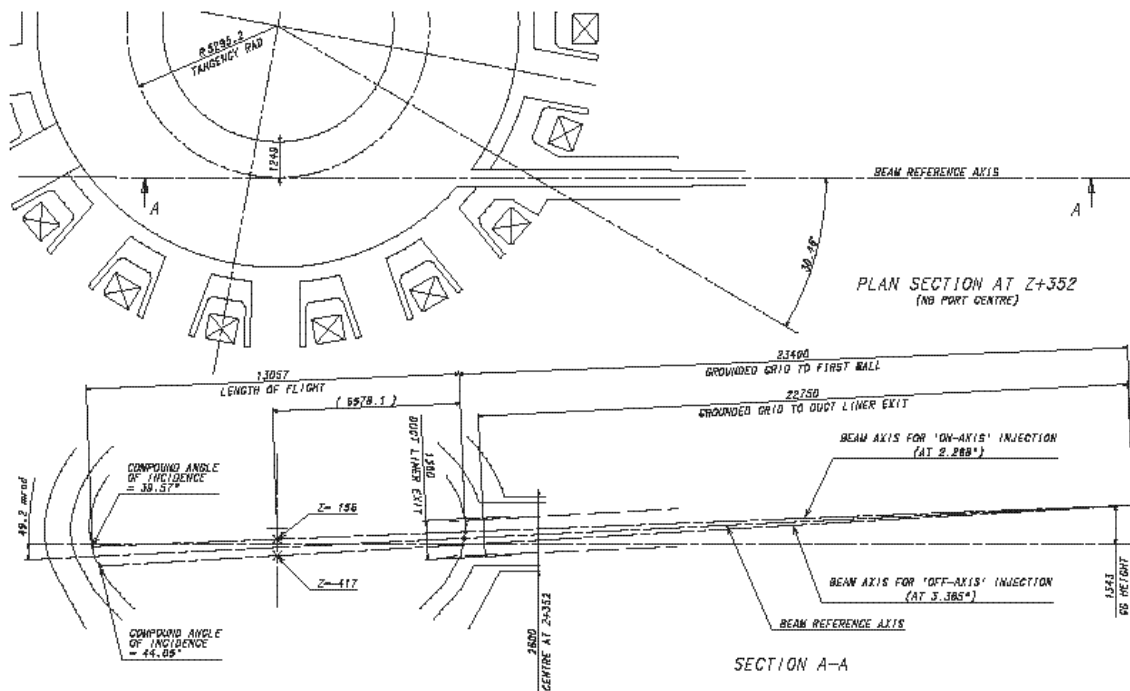


**Figure 2.5.1-2 Tokamak and H & CD Neutral Beam Geometry**

As the exact characteristics of the beam are unknown, the design has been done assuming a double Gaussian profile for the beamlets forming the beam with a core carrying 85% and with a halo carrying 15% of the beam. The divergence of the core is assumed to be in the range 3 – 7 mrad and the divergence of the halo is assumed to be 15 mrad. Existing R&D results support these assumptions. Moreover, maximum misalignments of 2 and 4 mrad have been added in the horizontal and vertical directions respectively. In considering the beam transmission and the power loading of the beamline components, the “worst case” combination of the assumed beam characteristics has been studied to ensure that the system meets the ITER requirements (see below).

The design of the channels of the neutraliser and of the RID is a compromise between gas flow and beam transmission requirements. In spite of the narrow channels, the NB injection power  $\sim 16.5$  MW and efficiency of  $\sim 35\%$  could be achieved even with the 7 and 15 mrad divergence of the core and of the halo respectively, plus 2 mrad horizontal misalignment (worst case).

The magnetic field produced by the tokamak in the spaces where the beam is formed and transmitted is  $\sim 20$  mT in the ion source and  $\sim 70$  mT at the calorimeter exit. A combination of passive shielding ( $\sim 0.15$  m thick) and active coils ( $\sim 200$  kA turn per coil), reduces the field in the beam volume to an acceptable value which is between 0.1 – 0.2 mT. Moreover the line integrated field from the beam source to the exit of the neutraliser (total length  $\sim 4$  m) should be  $4 \times 10^{-4}$  Tm to improve beam transmission.

### 2.5.1.4 Component Design

Figure 2.5.1-4 shows the beam source and HV bushing.  $D^-$  ions are extracted from an arc discharge produced between tungsten filaments (cathode) and the source body (anode). Small quantities ( $< 1$  g) of caesium are introduced into the discharge as this has been found to enhance the production of negative ions. The overall efficiency of the source is increased by a multi-cusp magnetic field created by permanent magnets on the source body. The plasma grid (PG) operates at high temperature, between  $250 - 300^\circ\text{C}$ , as this has been found to further enhance the negative ion production. A current is passed through the plasma grid ( $2 - 4$  kA), which generates a magnetic field (PG filter) that reduces the loss of negative ions by collision with fast electrons, and the number of extracted electrons. The plasma and extraction grids form the extractor (height  $\sim 1,540$  mm, width  $\sim 580$  mm). Each grid is made up of 4 horizontal segments, divided into 4 groups. Each group has  $5 \times 16$  apertures, so that the total number of apertures is 1,280.

N 53 GR 390 01-06-14 R 0.2

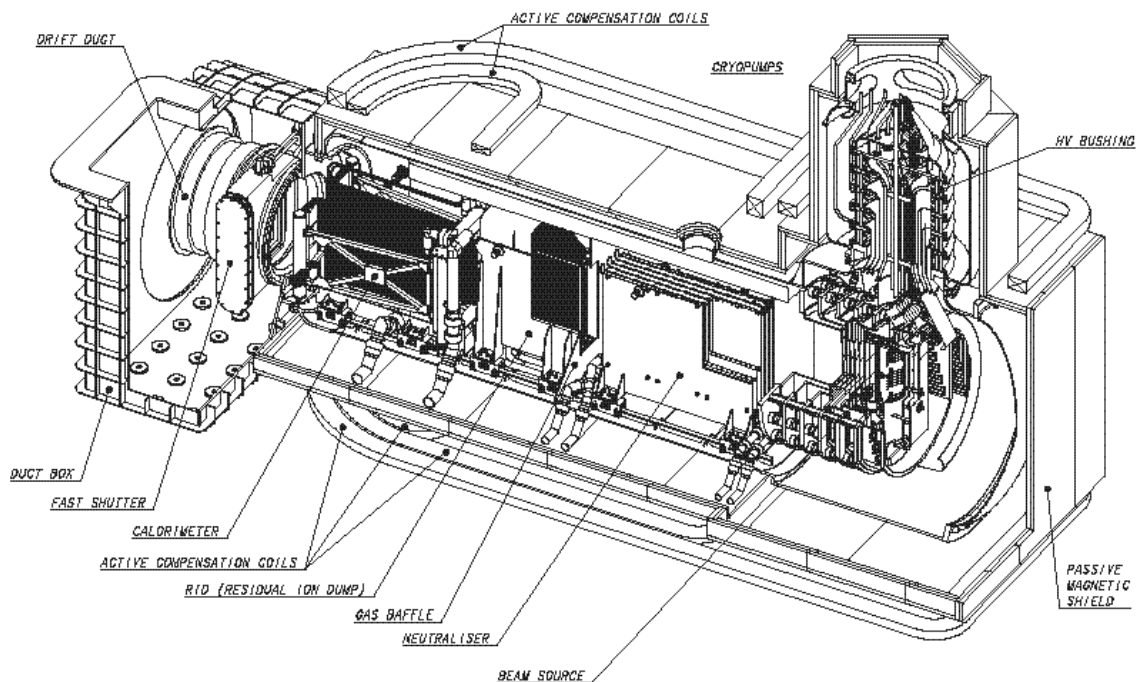


**Figure 2.5.1-3 Neutral Beam Injector, Isometric View**

R&D is in progress on two accelerators: the multi-aperture multi-grid concept (MAMuG) under development in Naka, and the single gap concept (SINGAP) under development in Cadarache. In the MAMuG concept, the accelerator consists of 5 stages, each stage consisting of 4 grid segments for beam aiming. Post insulators support the intermediate acceleration grids and the ion source. The design current of the negative ion beam, at the exit of the grounded grid, is 40 A. In the SINGAP concept, a pre-acceleration stage ( $\sim 30$  keV) follows the extractor, and this is followed by a single acceleration stage. The pre-acceleration grid is similar to those of the MAMuG accelerator with an identical aperture pattern. In the acceleration stage, beamlets from one group of apertures are merged and

accelerated through a single aperture in the final grid. MAMuG is the more conservative extrapolation from experience in positive ion accelerators and electrostatic particle accelerators, and has been considered the basis for the ITER design.

The beam source is in the primary vacuum. The reason for vacuum insulation is to remove the problem caused by the radiation induced conductivity (RIC) in the high pressure gas insulation present in the previous design. Vacuum insulation provides an additional advantage: lateral pumping, through the spaces between the post insulators, reduces the stripping loss of the ions in the accelerator to 25% (instead of 43%). Low stripping losses are the main reason to operate the ion source with low D<sub>2</sub> filling pressure 0.3 Pa.

The primary vacuum is sealed by a 1 MV, five stage bushing made up of two coaxial insulators: the inner, facing the vacuum, in ceramic (1.56 m outer diameter, OD), and the outer, facing SF<sub>6</sub> gas, in fibre-reinforced plastic (1.76 m outer diameter).

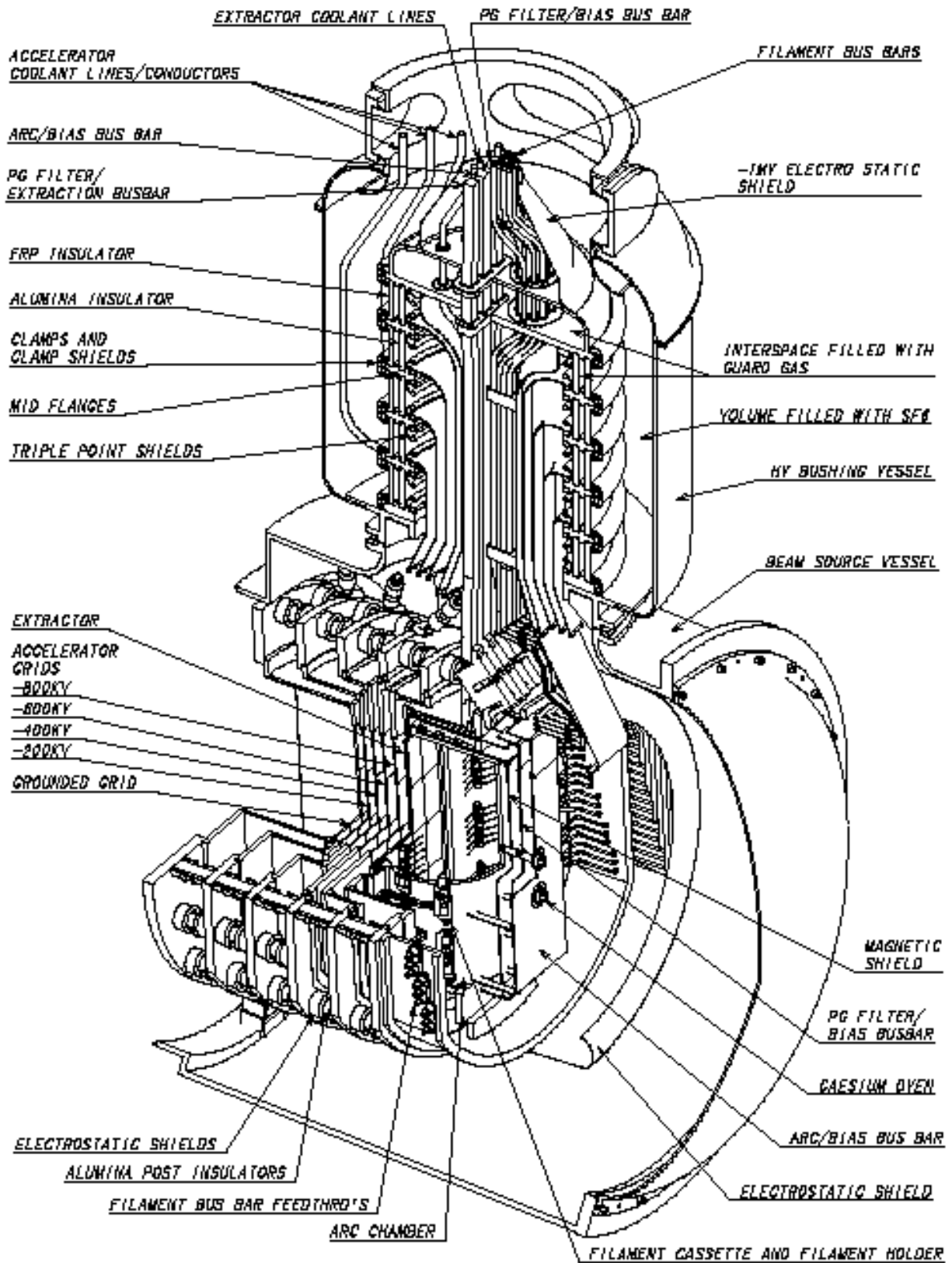
The space between the two insulators is filled with “guard gas“ to avoid contamination of the primary vacuum with SF<sub>6</sub>. The guard gas could be nitrogen or dry air. Electrostatic analysis of the HV bushing and of the beam source is in progress, and R&D in the JA home team is underway to refine the design criteria. The ceramic insulator with 1.56 m OD is technically challenging, but, in principle, within the present capability of industry.

The gas neutraliser provides ~ 60% neutralisation efficiency for the 1 MeV D<sup>-</sup> ions. The beam, at the exit from the neutraliser, consists of neutrals and residual ions (D<sup>-</sup> and D<sup>+</sup>, each ~ 20%). In the worst case (7 mrad core divergence plus 2 mrad horizontal misalignment) the maximum power deposited on the walls of the neutraliser channels is 4.2 MW and on the neutraliser leading edges is 370 kW; there the maximum power density is 2.1 MW/m<sup>2</sup>.

The residual ion dump (RID) uses an electric field to deflect the ions that are dumped on the five RID panels. The field is produced by applying zero potential to the odd panels (the two external and the central panels) and - 20 kV to the two even panels. In the worst case (7 mrad core divergence plus 2 mrad horizontal misalignment) the maximum power deposited on the RID panels is 19.6 MW. The maximum power density that could be encountered, 6.0 MW/m<sup>2</sup>, occurs if the beam core divergence is 3 mrad.

A movable calorimeter intercepts the neutral beam during the commissioning and conditioning phases. A single V-shaped calorimeter is selected. The maximum power deposited in the panels of the calorimeter, 21.6 MW, and the maximum power density, 22 MW/m<sup>2</sup>, arise if the beam core divergence is 3 mrad. The calorimeter panels consist of an array of swirl tube elements, parallel to the beam direction. A limited deflection of the swirl tube array (about 40 mm) can be allowed, and the secondary stresses can be limited to < 200 MPa.

The neutraliser, the RID and the calorimeter are water-cooled. Swirl tube elements made of CuCrZr-alloy are foreseen in the RID, the calorimeter and in the neutraliser leading edge. The overall design guarantees acceptable thermal fatigue of these components throughout the operation life.



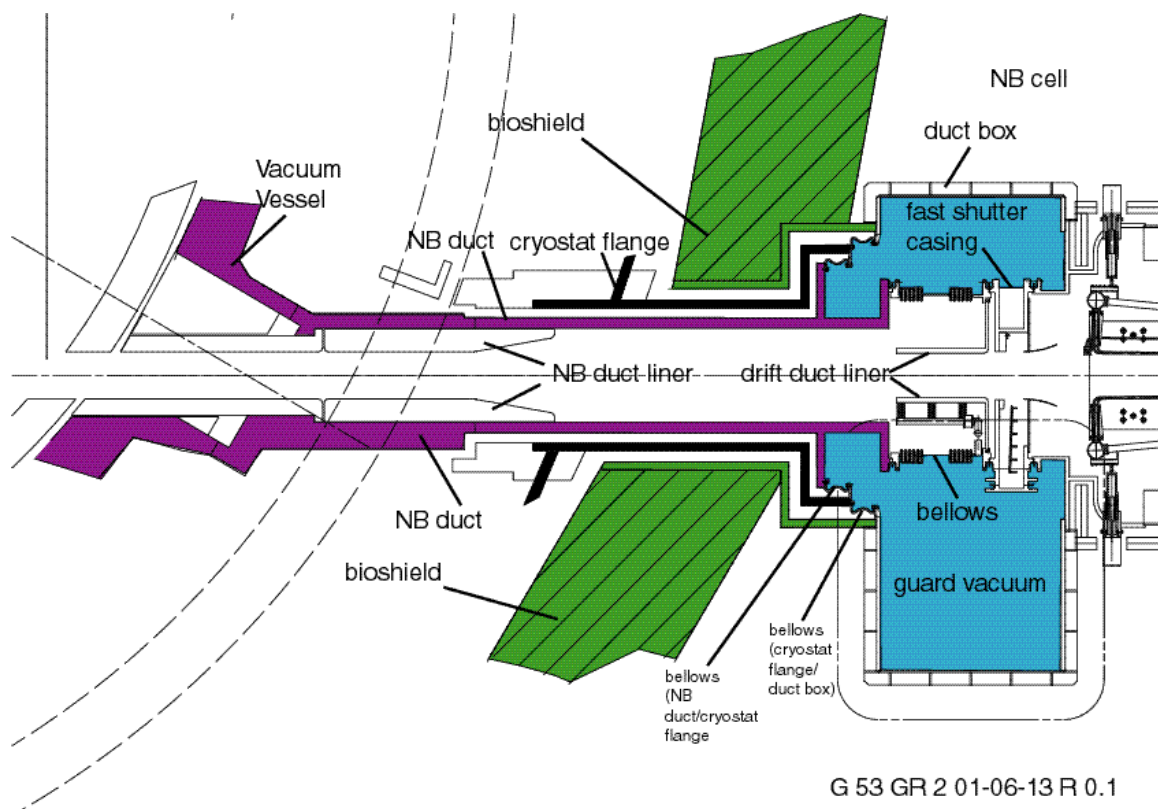
N 53 GR 392 00-11-22 W 0.1

Figure 2.5.1-4 H&amp;CD NB: HV Bushing and Beam Source

Large cryopumps maintain low pressure in the injector outside the ion source and the neutraliser. They are located close to the wall of the beam line vessel from the entrance of the neutraliser to the exit of the calorimeter. They cover all but the lower section of the beam line vessel where the support structure of the beam line components is located together with the coolant and the gas supply lines. The surface allocated to the cryopumps is about 47 m<sup>2</sup> and the assumed absorption probability for the cryopumps is 0.2. A gas baffle is mounted at the RID entrance to subdivide the injector volume and therefore to achieve differential pumping.

The injector is contained inside two large pressure vessels: the beam source vessel and the beam line vessel. Both are designed to guarantee the confinement of radioactive materials in case of an accidental overpressure: they are designed for a maximum internal pressure of 0.24 MPa (absolute pressure).

A “fast” shutter is located at the exit of the injector vacuum vessel to prevent tritium flowing from the torus to the injectors and to allow regeneration of the injector cryopumps without significantly increasing the torus pressure. This is essentially a lightweight “door” which can be moved across the beam path to seal against a frame built into the exit of the beam line vessel. A flexible metal seal on the frame ensures a low conductance between the injector and the torus of  $10^{-4}$  m<sup>3</sup>/s for D<sub>2</sub>.



G 53 GR 2 01-06-13 R 0.1

**Figure 2.5.1-5 H&CD NB: Connections to the NB Duct and Cryostat Flange**

The drift duct is the last component of the NB system and allows the flexible connection between the fast shutter casing (connected rigidly with the beam line vessel) and the NB duct (Figure 2.5.1-5), connected rigidly with the vacuum vessel. Two bellows with equalizing rings connected with an intermediate cylinder are foreseen between the two extremity

flanges. The drift duct liner faces the beam and protects the two bellows. The duct box encloses the fast shutter and the drift duct and provides a double barrier, with guard vacuum, between the NB cell and the primary vacuum. It provides also the nuclear shielding in this region.

The magnetic field reduction system consists of a passive magnetic shield and of active compensation and correction coils. The passive magnetic shield (PMS) encloses the beam line and the beam source vessels, the HV bushing, (and maybe the transmission line and the HV deck). Its purpose is to reduce the magnetic field in the space inside it, and the radiation (neutrons, gamma and X-rays) in the space outside it. The PMS is made of ferromagnetic steel with 150 mm thickness. It is a simple structure made of two construction steel plates each 75 mm thick, bolted together. Six active compensation coils (three above and three below the PMS) limit the flux in the space inside the PMS and reduce the field in the PMS below its saturation value. Finally, an active correction coil, located between the beam line vessel and the fast shutter, could limit, if required, the error field produced by the NB system on the plasma. All coils are made of copper and are water-cooled.

#### 2.5.1.5 Diagnostic Neutral Beam

The main parameters (Table 2.5.1-2) of the diagnostic neutral beam (DNB) have been progressively identified, as a trade-off between diagnostic requirements and engineering feasibility. The beam is injected in a series of modulated “pulse trains” with the repetition time given in the table.

**Table 2.5.1-2 Diagnostic Neutral Beam, Main Parameters**

Parameter	Unit	Value
Accelerated ion		H <sup>-</sup>
Beam energy	keV	100
Injected neutral (H <sup>0</sup> ) equivalent current	A	20
DNB pulse train duration	s	up to 3
DNB pulse train modulation frequency	Hz	5
Modulation wave form		Square (100 ms on/100 ms off)
Repetition time	s	20
Integrated number of pulse trains		1.0 x 10 <sup>6</sup>
Integrated number of modulations		1.5 x 10 <sup>7</sup>

The overall design concept of the DNB injector is identical to the one used for the H&CD injectors. This allows to utilise most of the R&D and design performed for the H&CD injectors and to standardise the components, maintenance equipment and procedures.

In the beam source, one single stage of acceleration is used. The design assumes 300 A/m<sup>2</sup> as the accelerated current density of H<sup>-</sup> corresponding to a total accelerated current of 60 A. For the beam optics and misalignment, the same assumptions are made as for the H&CD injectors.

The requirements for the magnetic field reduction system are about a factor 4 more stringent than in the H&CD injectors, due to the lower beam energy. The line integral of the residual

magnetic field in the space between the accelerator grounded grid and the neutraliser exit (about 4 m) has to stay at the level of  $1 \times 10^{-4}$  Tm.

The mechanical design of the neutraliser is similar (4 vertical channels) to the one used for the H&CD injectors, apart for minor differences related to the beam aiming. The same neutralisation efficiency of about 60% can be achieved.

A RID is used for the deflection of the ions ( $H^-$  or  $H^+$ ) exiting the neutraliser. The RID length is 1 m and the required deflecting voltage is limited to 4 kV. During “beam on” time the peak power density on the RID panel is about  $0.75 \text{ MW/m}^2$  and total power to the RID is about 2.5 MW. Utilising, for the mechanical design of the RID, the same concept of the H&CD injector RID, the thermal fatigue limits are satisfied.

During “beam on” time the peak power density at the calorimeter position is  $12 \text{ MW/m}^2$  (normal incidence) and total power is about 3.5 MW. The power is accommodated by a movable calorimeter with a heat receiving panel inclined  $45^\circ$  with respect to the beam line axis. Peak power density on the panel surface is about  $8 \text{ MW/m}^2$  and, utilising the same calorimeter design concept as for the H&CD injectors, the thermal fatigue limits are satisfied.

The blanket segmentation, the DNB duct neutron shielding, and the clearance with the toroidal field coil structures, determine the vertical position of the DNB axis ( $Z = +1,070 \text{ mm}$ ).

#### 2.5.1.6 Maintenance

The NB system will become activated by neutrons streaming directly into each injector and the system will need to be remotely maintained. The whole (remote handling class 3) system does not need maintenance in the lifetime of ITER except for the following.

- The filaments of the ion source (class 1) have a finite life, estimated as  $> 200 \text{ h}$ . They should be replaced twice a year (or less) through the rear formed head of the beam source vessel.
- The caesium oven (class 1) will need to be replaced; this operation is expected to take place every two years.
- Caesium will flow from the ion source to the accelerator and may eventually contaminate the insulator, which might require cleaning. Its frequency is expected to be less than once per year. If this cleaning cannot be carried out in situ, the removal of the source will be required (class 1). This complex procedure has already been studied and considered feasible (see 2.9).
- The fast shutter requires maintenance for seal wear (class 2).

#### 2.5.1.7 Design Assessment

The design is based on the R&D targets which are summarised below and compared with the main results achieved so far.

##### *Ion Source*

$200 \text{ A/m}^2$  of  $D^-$  have been extracted and accelerated ( $\sim 27 \text{ keV}$ ) for short pulses (5 s) with the arc discharge lasting 150 s in a source with filling pressure of 0.30 Pa. However, the stripping loss in the 1 MeV accelerator will be significantly higher than in the low energy accelerator used for the R&D. Hence the R&D needs to demonstrate  $\sim 250 \text{ A/m}^2$ , to achieve

the required current density at the grounded grid of the ITER accelerator. Moreover continuous pulses of 1,000 s should be produced repetitively and reliably. These are the targets for the R&D in progress. The demonstration of an acceptable source uniformity ( $\pm 10\%$ ) is also essential in an ITER source.

### *Accelerator*

Experiments in the EU and JA home teams with high energy beams with ITER-relevant current densities have been stopped since December 1998; studies in the beam optics are still at relatively low energies (700 – 860 keV). The main reason has been failures in both test beds of the large cylindrical insulators made of epoxy. These failures were caused either by faulty manufacturing (EU) or outgassing from the fibre-reinforced epoxy to the vacuum (JA). Outgassing of epoxy is irrelevant in the ITER design of the HV bushing (described above), as this has ceramic facing the vacuum and compressed gas on both sides of the epoxy secondary insulator.

The JA HT succeeded in 1 MeV acceleration of  $H^-$  ions but at a very low (a few  $A/m^2$ ) current density (hence with poor optics). The EU HT achieved  $D^-$  ion acceleration up to 630 keV at  $53 A/m^2$  and  $H^-$  ion acceleration up to 860 keV at  $36 A/m^2$ , with good optics in both cases. The main targets of the 1 MeV accelerator R&D are to demonstrate 1 MeV negative ion beams at the same perveance conditions of  $\sim 0.5 A, 280 A/m^2 H^-$  (MAMuG) and of  $\sim 0.1 A, 200 A/m^2 D^-$  (SINGAP). Demonstration of the reliability of such beams (each with pulse length of  $\sim 1 s$ ) is one of the targets.

The R&D in progress on these key aspects has to continue with increased effort after the end of the EDA until the targets are achieved. The experimental results obtained in the last two years have been too limited to be appropriate to the challenges ahead.

## **2.5.2 Radio-Frequency Systems**

### **2.5.2.1 General Design Features of the RF Heating and Current Drive Systems**

The design of the radio frequency H&CD systems has been developed with the aim of providing for all systems:

- a credible high-level power performance associated with a high reliability;
- modular construction and identical interfaces wherever possible;
- interchangeable in-vessel assemblies;
- standardised control systems (with an unique man-machine interface) and operation.

### **2.5.2.2 Layout**

The RF H&CD systems use different power generation and transmission components, but have similar general layout. The one of the ion cyclotron system, shown in Figure 2.5.2-1, is used as example, to identify the common components.

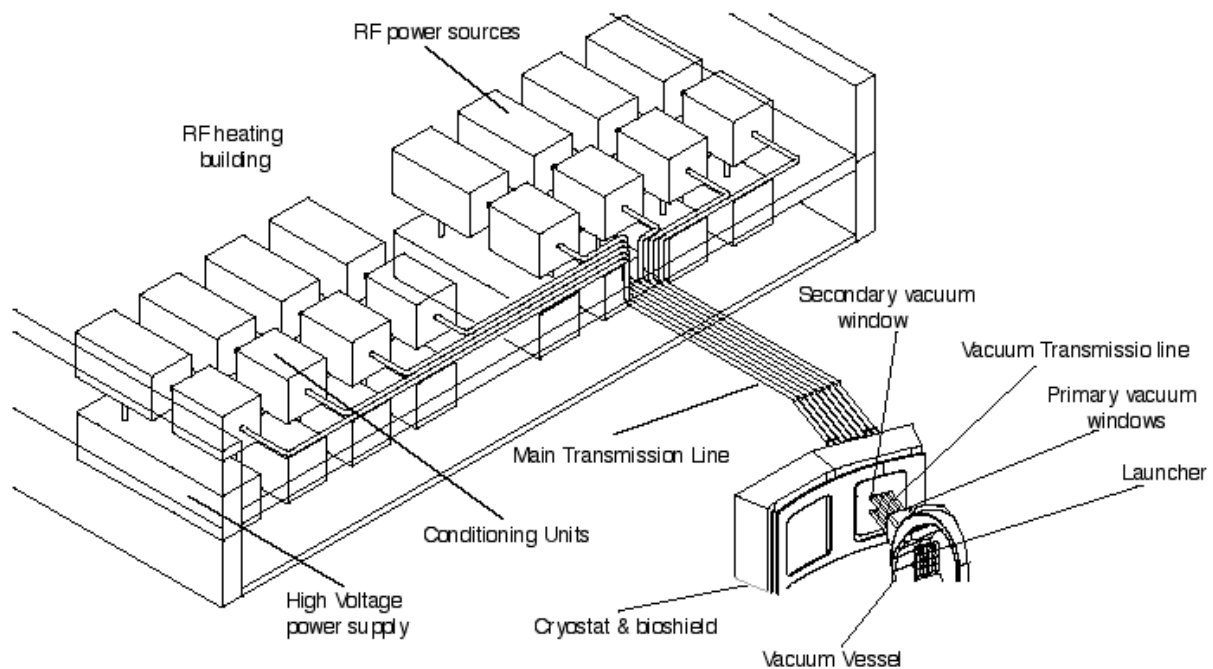


**Figure 2.5.2-1IC System Layout as Example of RF System Layout, Showing the Relative Locations of i) Launcher, ii) Primary and Secondary Vacuum Windows, iii) Vacuum and Main Transmission Lines and iv) Power Sources.**

The RF launchers are designed as interchangeable plugs inserted in the vessel equatorial ports, featuring:

- the same nominal installed power per port (20 MW/port), corresponding to an average power density of  $9.2 \text{ MW/m}^2$  at the plasma boundary;
- the same neutron shielding /activation performance;
- the same confinement boundaries and interfaces with the VV port;
- the same remote maintenance requirements, interface and procedures.

Four equatorial ports can be used to provide a maximum RF power of  $\sim 80 \text{ MW}$ ; two are expected to be used for the initial experiments.

Smaller EC launchers ( $\sim 7 \text{ MW/port}$ ), specialised for NTMs stabilisation, are integrated in four upper ports. The general layout of the upper launchers is similar to the one described, but with different geometry and dimensions.

The launcher assemblies of all RF systems are supported by the same mechanical structure sketched in Figure 2.5.2-2.

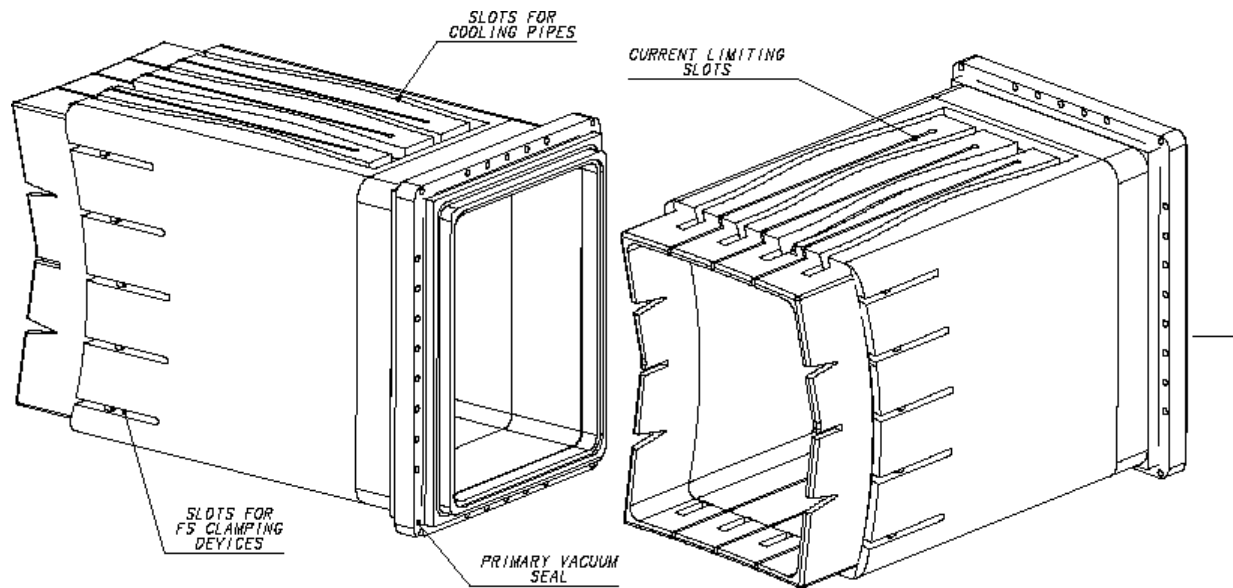


**Figure 2.5.2-2 Front and Back of RF Assembly Support Structure, Including Port Flange and Closure Plate**

The support structure of the launcher includes the vacuum vessel port closure plate, which transfers to the port the gravity load and the bending moments induced by plasma disruptions. The structure is also used to distribute coolant to the different RF components from blanket and VV cooling loops. The support structure is not in contact with other in-vessel components.

A gap of 20 mm is allowed from the port walls all around the plug perimeter and an overlap of 30 mm is provided by the adjacent blanket modules, to shield direct neutron streaming in the gap. A gap of 120 mm is allowed between plasma separatrix and the first wall in equilibrium conditions at the outboard equator.

The first wall of the RF launcher assemblies is designed to accept the same thermal loads from plasma radiation and neutrons as the adjacent shield blanket modules. However, they are not designed to be exposed to conduction heat loads from the plasma (e.g. during the start-up phase) from which they are protected either by the blanket or by shielding structures built in the blanket.

The RF launchers include a neutron shield, about 1 m thick, which reduces the high energy ( $E > 1$  MeV) neutron flux outside the VV closure plate to  $1.18 \times 10^7$  n/cm<sup>2</sup>s, and limits the integrated activation level in the area to produce  $< 100$   $\mu$ Sv/h, 15 days after shut-down. Hands-on maintenance of the components in the port inter-space would be therefore permitted. The neutron shield is penetrated by wave-guides and transmission lines of type specific to the different frequencies. Artificial bends (doglegs) are included in their path, to reduce the radial neutron streaming.

Plasma-facing components and neutron shield are cooled in parallel by pressurised water distributed by the blanket cooling loop. The coolant manifolds are located within the support structure. The closure plate and the components integrated in it (e.g. windows) are instead connected to the VV cooling loop.

The boundary of the primary vacuum confinement is located at the closure plate of the vacuum vessel, and the secondary boundary is at the cryostat closure plate. Water-cooled ceramic windows are used in each wave-guide or coaxial line. The dielectric window materials are different in different systems: BeO is used for IC and LH and polycrystalline diamond for EC.

Sections of evacuated waveguide/transmission line (VTL) join the vacuum vessel closure plate to the cryostat closure plate and penetrate the bioshield (vacuum transmission line). The vacuum transmission lines are manually disassembled, to allow remote-handling cask to dock to the VV port.

Monitoring and safety-related equipment is installed at the end of the VTL, in locations easily accessible for maintenance. Among others, DC breaks (to prevent ground loops being closed outside the pit) and rupture disks, exhausting in the volume served by the detritiation system, are installed.

Outside the bioshield, the VTLs are connected to the main transmission lines (MTLs). These run on the ceilings of the appropriate port cells and gallery, and are then routed to the RF heating area of the laydown, assembly and RF heating building.

For continuous operation, VTLs and MTLs are water-cooled by loops of similar specifications, connected to the cooling water system (see section 3.3). The MTL of IC and LH use a pressurised gas as waveguide dielectric, whereas the EC lines are evacuated.

The RF power sources (gyrotron oscillators for EC, gridded-tube amplifiers for IC, and klystron amplifiers for LH) are connected to the MTLs by RF conditioning and matching components. In the case of LH, the power of four klystrons is combined, to minimise the number of transmission lines.

The RF power sources are connected to their main DC supply, located at grade in the RH heating area of the laydown, assembly and RF heating building when a voltage fault is detected. Fast protection rapidly ( $10\ \mu\text{s}$ ) removes the DC supplies to prevent arc damage in the tubes. In view of the long pulse operation, the protection is designed for multiple response and power re-application, after a time suitable for the arc to clear.

### 2.5.2.3 Electro-mechanical Analysis

Owing to the similarity of the mechanical layouts, the electromechanical analyses of the three RF launchers have been performed using the same finite element model, by simply varying the electrical and mechanical properties of the material(s) according to the individual design. A harmonic analysis at 10 Hz frequency has been performed.

The spatial distribution of the disruption-induced currents in the assembly is computed first, from local poloidal and radial magnetic flux variations, inferred from global magnetic field analysis. The intensity of the eddy current is reduced, and their distribution modified, by the introducing radial cuts in both neutron shield and support structure. Different segments are either insulated or electrically connected by low value (typically 0.1-1 m $\Omega$ ) carbon fibre composite resistors. The results of the analysis are:

- the 3D map of resistive and inductive currents;
- field distribution in assembly metal and voids;

- loads applied to the port closure plate;
- stresses applied to the different assembly components.

In Figure 2.5.2-3a) a stress/strain map computed for the whole IC launcher is shown.

In Figure 2.5.2-3b) a stress analysis output of a section of the EC support structure is shown.

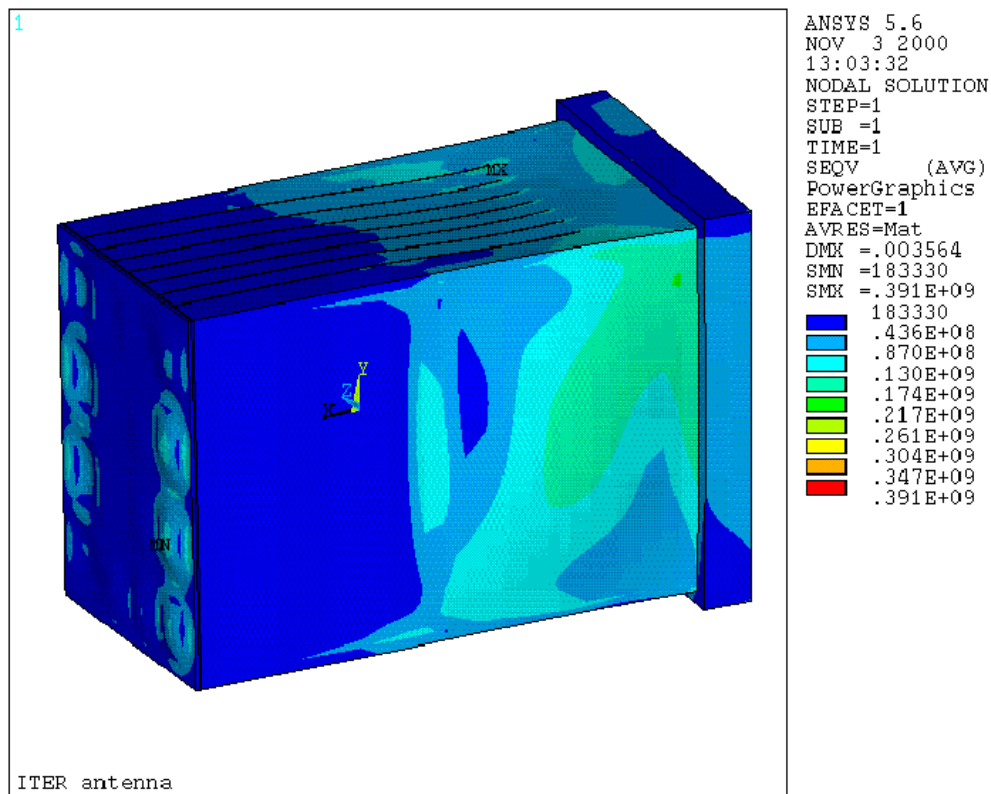


**Figure 2.5.2-3(a)**  
**Example of IC Launcher von Mises Stress and Strains Map**

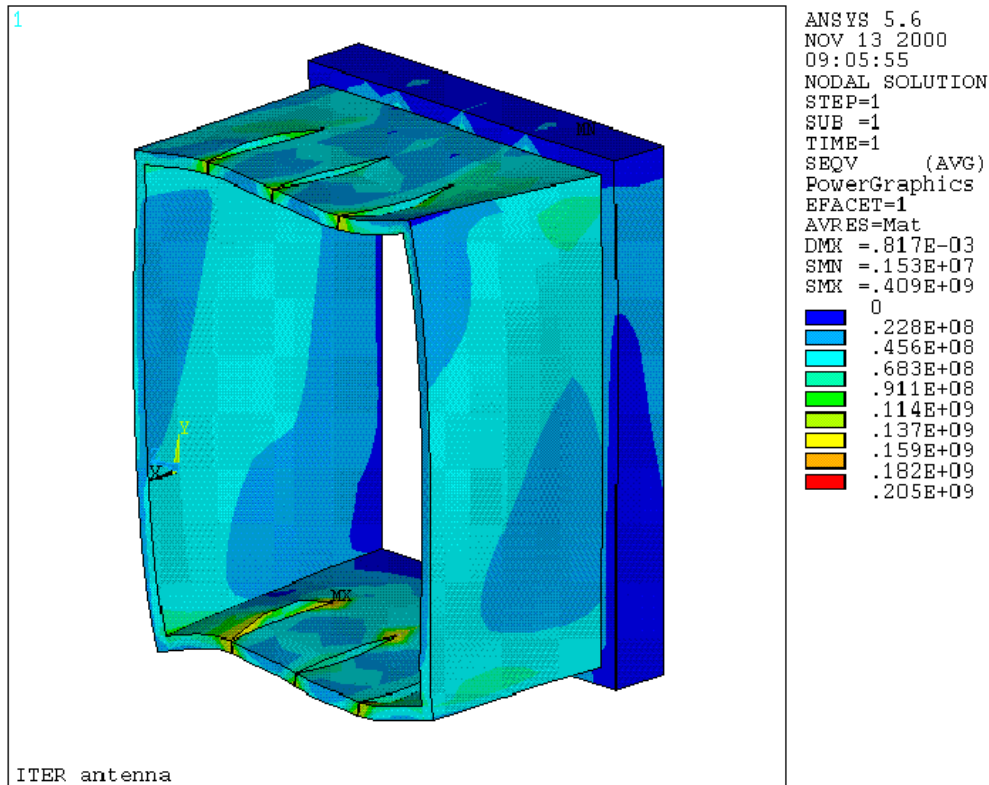


**Figure 2.5.2-3(b)**

**Von Mises Stress and Strain Map in a Section of the EC Support Structure**

A summary of the stress analysis is reported in Table 2.5.2.3-1. These comply with the limits set by the structural requirements for the equatorial ports.

**Table 2.5.2.3-1**  
**Typical Forces and Moments Applied by RF Launcher to the VV Port**

Parameter		EC	IC	LH
Radial force	(MN)	-0.93	-0.149	-0.169
Poloidal force	(MN)	-0.165	-0.194	-0.195
Toroidal force	(MN)	0.010	0	0
Radial moment	(MNm)	7.09	5.89	11.99
Poloidal moment	(MNm)	-2.22	-1.53	-2.62
Toroidal moment	(MNm)	0.18	-0.92	-0.14
Max current (kA)		1.070	0.409	0.839
		in Farad. Shield	in Closure Plate	Launcher Front
Max deformation (mm)		0.3	0.4	0.8
Max von Mises stress in SS (MPa)		90	80	120

**2.5.2.4 Commissioning and Operation**

The in-vessel components of the RF systems are delivered from the manufacturer fully assembled, conditioned for high vacuum and leak-tested at room temperature. Their integration in the port requires installation and vacuum sealing of the closure plate.

For initial commissioning and acceptance tests, and for commissioning tests after refurbishment in the hot cell, the RF systems share the use of a test stand (TS). The TS is a vacuum vessel having dimensions and shape similar to the ITER VV port and can accommodate any of the RF launcher assemblies. It is provided with a flange mating with the port closure plate, and encloses test loads. The test stand is installed in the hot cell, to allow testing on activated equipment.

The RF H&CD systems require a large number of RF and low frequency monitoring channels, control functions and protection circuits. However, monitoring and control functions of the three RF systems are very similar. They can be implemented by a single set of standardised procedures for data handling, control, alarm handling and machine-man interface.

The operation is co-ordinated by a plant control system, responsible for all real time control/monitoring transactions, which reports in real time to the ITER CODAC system.

Three basic states of operation are possible.

- In the normal state of operation, the RF output power is equal to the pre-set power and all other system parameters are within their operational windows.
- The control system switches to power limit operation if one or more system parameters indicate abnormal operating conditions. The RF output power of that system is automatically reduced to the highest level compatible with the current parameter state and is automatically restored when the limiting parameter recovers the normal value. The RF power of the other systems is increased, to compensate the missing power.
- The RF output power of one of the system is temporarily suppressed during a power trip, to allow abnormal load conditions (such as an arc) to clear. The RF power (and in some cases the DC high voltage) is rapidly removed ( $\sim 10 \mu\text{s}$ ), to prevent a large energy being dissipated in the fault, and reapplied through an "intelligent" routine, to avoid re-strikes. The RF power of the other systems is increased, to compensate the missing power.

#### 2.5.2.5 Maintenance

The RF in-vessel assemblies are designed to make maintenance simple in situ and in the hot cell. The use of a single support structure automatically makes all interfaces with the vessel identical, and standardises remote handling equipment and procedures.

The launcher assemblies are designed to allow a RH cask to dock to the VV port, after the manual disconnection of vacuum transmission lines, water cooling pipes and pumping ducts. They are installed in, and removed from the VV port, using standard RH procedures, and transferred by cask to the hot cell.

Hot cell maintenance is meant for:

- i refurbishment of damages to plasma-facing sections (such as EC shield, IC Faraday shield, LH outer multi-junction stack. To this purpose, all plasma-facing components are separable from the assembly;

- ii preventive maintenance or replacement of defective components. The most critical components (such as mirrors, tuners, actuators and windows) are located either on the front sections or installed on the closure plate using standard flanges. Maintenance is performed by complete substitution, needing disassembling and re-welding of the substitute.

The RF launcher assemblies are themselves modular in construction, and can be disassembled into mechanical subsets having weight lower than 10 t. The elements composing an IC launcher are shown in Figure 2.5.4-4.

The waveguide/transmission lines located within the secondary vacuum boundary and those running at atmospheric pressure are commercial components of different types (coax transmission (IC), rectangular wave-guide (LH) and circular, corrugated wave-guide (EC). Transmission lines and power sources are commercial items. Maintenance of these is performed according to the manufacturer's user manuals.

#### 2.5.2.6 Design Assessment

The design of the RF systems outlined below underlines engineering solutions that meet ITER physics requirements and are consistent with the current technologies.

The design effort has mainly focussed on assessing the capability of the in-vessel components of surviving and safely operating in the reactor environment. Operational issues, (such as the way of efficiently fulfilling the requirements of an integrated real-time control, protection and data management system, in quasi-continuous operation), have been generically addressed, as they are likely to benefit from future technology advances.

The level of design development is similar for the three systems. The launcher design is still at a conceptual level in some case (e.g. the remote steering design for EC, and the PAM stack for LH still need demonstration). However, for most components, and in particular for those directly facing the plasma, no showstoppers have been identified and there is sufficient information to start manufacturing drawings.

Manufacturing processes were only generically addressed for costing purposes. The technology developed for the first wall and blanket are however generally applicable to the RF plasma-facing components.

Specific R&D programs did not investigate the launcher design specifications. A limited development of mock-ups and high power tests in vacuum was carried out for the IC system launcher (and is still ongoing), and has confirmed the design parameters<sup>1</sup>.

The status of development of the power sources is different for the three systems. The 170 GHz, CW, 1 MW, 50% efficiency gyrotron development programme for the EC system is still far from meeting ITER specification. The best results achieved at this frequency are: 8 s pulse length, 0.45 MW and 33% efficiency. For IC, an industrial study has shown that a source fulfilling ITER specification (2 MW-CW-40/60MHz at a VSWR < 2.5) could be constructed using existing tetrodes, although an upgrade of a current tube would lead to a more cost effective source. There are no detailed studies of a 1MW-CW-5 GHz klystrons.

---

<sup>1</sup> ITER/US/98/IV-RF-01(T361 US) Final report

Finally, it should be always kept in mind that the operation of both IC and LH launchers is plasma dependent. Plasma edge parameters and separatrix distance need to be controlled at the antenna(s), for an efficient power transfer and to reduce to the very minimum RF losses in the plasma edge, which could otherwise cause wall loading and release of impurities unacceptable for long pulse operation.

It has not proved possible to test RF launcher features on plasma or in otherwise ITER-relevant operating conditions.

The R&D on these key aspects, have to be addressed after the end of EDA until all design parameters are demonstrated. These key aspects are all important and difficult targets, which need an efficient organisation and will to be achieved.

### **2.5.3 Electron Cyclotron System**

#### **2.5.3.1 General Design Features**

The EC system uses two types of RF launchers, both operating at a frequency of 170 GHz. One type, located in an equatorial port, has toroidal beam steering capabilities ( $\pm 12.5^\circ$ ). The launcher is used for heating and current drive, with a typical on-axis CD efficiency is  $\eta_{20} = 0.2 \times 10^{-20} \text{ A/Wm}^{-3}$  and to assist start-up at a lower frequency (120 GHz). The other type is located in an upper port, and has poloidal RF beam steering capability ( $\pm 5^\circ$ ). This system is mainly used for neo-classical tearing mode (NTM) stabilisation, with the beam, and focussed at resonant flux surfaces ( $q = 2, 3/2$ ) in a position vertically off-set from the magnetic axis. This allows the use of a single frequency (170 GHz) for H&CD and NTM stabilisation and avoids higher harmonic power absorption during far off-axis CD when the main H&CD is applied. As an example of its use, the density of the driven current is plotted in Figure 2.5.3-1 for an equatorial launcher of 20 MW.

The nominal injection power is 20 MW at 170 GHz and 2 MW at 120 GHz. The RF power at 170 GHz is switched between the upper launcher and the equatorial launcher by changing of waveguide connections as shown in Figure 2.5.3-2. The RF power used for the assisted start-up is transmitted by three waveguides also used for the main H&CD. The power sources at 120 and 170 GHz are switched during a plasma discharge.

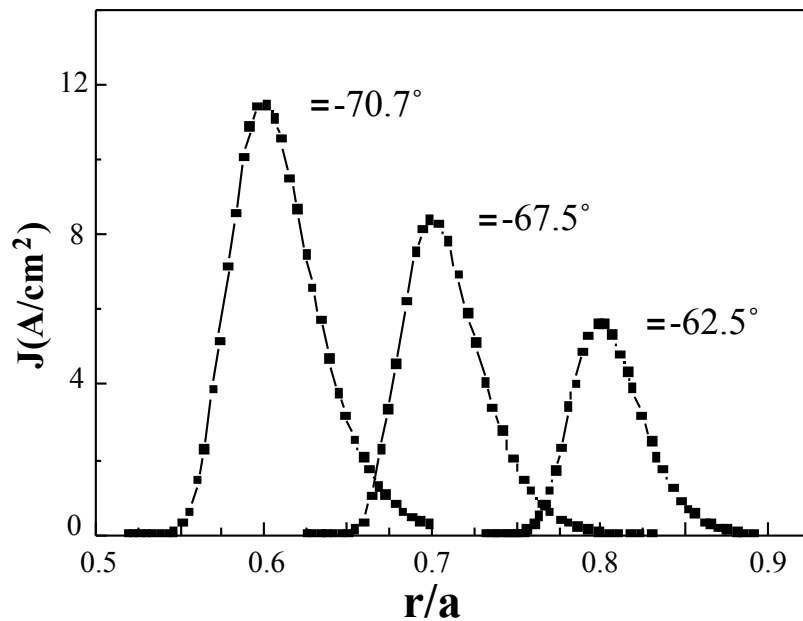


**Fig.2.5.3-1 Profiles of Driven Current vs. the Normalised Minor Radius**  
 Injected RF power is 20 MW and  $\theta$  is the angle between the beam and the horizontal plane, at an angle of  $24^\circ$  between the beam and the poloidal cross-section)

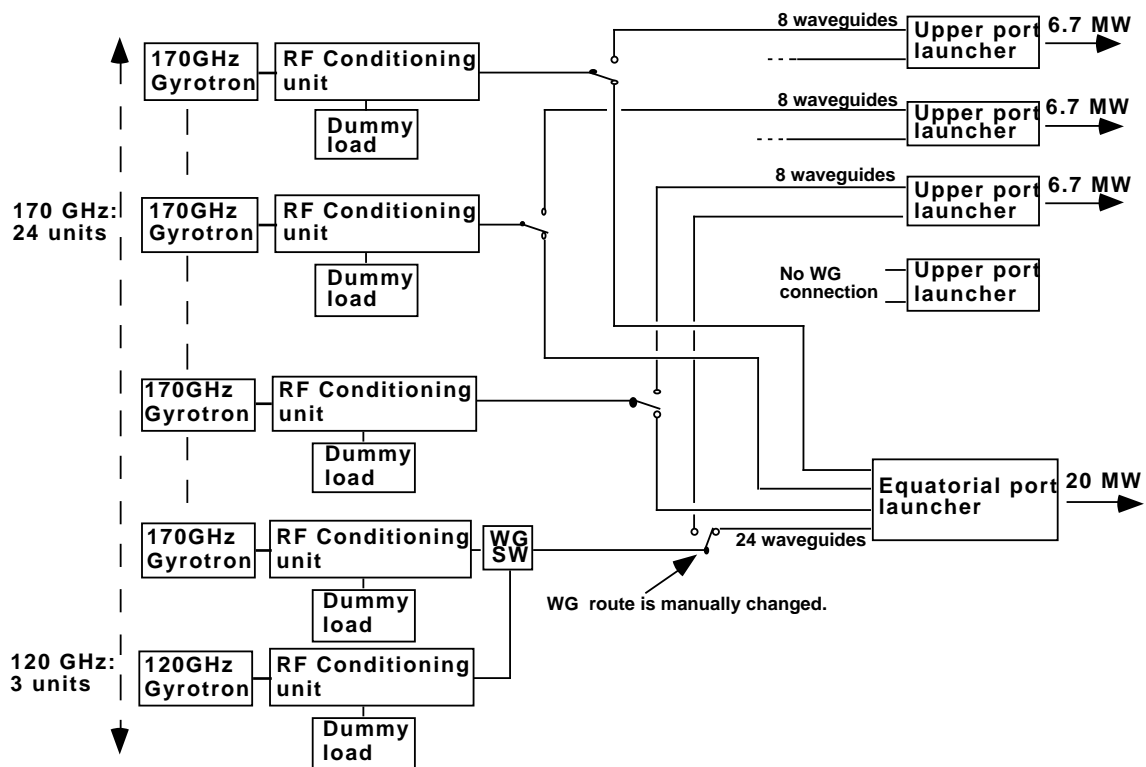


**Figure 2.5.3-2 Combination of Launchers and Gyrotrons**

### 2.5.3.2 Launcher(s) Design

There are three upper launchers and one equatorial launcher.

The equatorial launcher (Figure 2.5.3-3a) consists of i) a plasma facing neutron and radiation shield, ii) 3 sets of steerable mirrors, collecting 8 RF beams each, iii) 24 circular corrugated wave-guides, iv) mitre and v) diamond window.

The front shield has 3 horizontal slots and is segmented into modules. The steerable mirrors are made of dispersion strengthened Cu and supported by a pivot mounted on bearings. The mirrors are water-cooled to accommodate RF power losses (about 50 kW/mirror for a Be deposit of several  $\mu\text{m}$  thickness on the mirror surface), plasma radiation and nuclear heat.

A stainless steel spiral pipe having a mean diameter of 15 cm, a pipe inner diameter of 8 mm and a pipe thickness of 1 mm is used to supply the coolant to the steerable mirror. A shaft, operated by a pneumatic actuator, drives the pivot, and rotates the mirror without the need of links and cams. Plasma disruption currents induced in the spiral pipes and in the mirror, can be reduced to an acceptable level by electrically insulating the bearings.

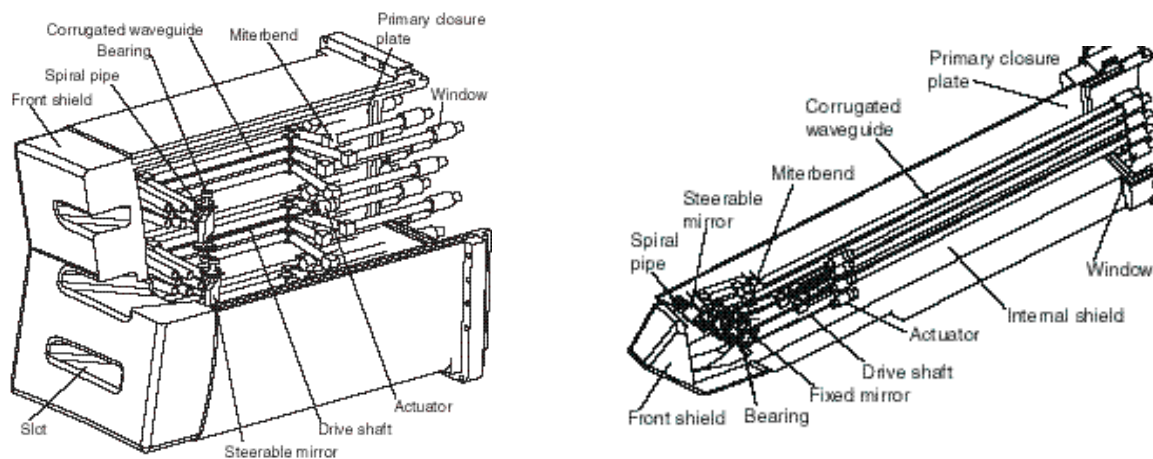


**Figure 2.5.3-3 a) Equatorial Launcher  
b) Upper Launcher (Front-steering Type, see Text Below)**

The in-vessel waveguides must include a dog leg in order to avoid excessive radial neutron streaming and satisfy the maintenance dose rate requirement at the primary closure plate. Electrically insulated mitre-bends are used in these sections. These components need water cooling.

A diamond disc obtained by chemical vapour deposition (CVD)<sup>1)</sup> is used in each line as a primary vacuum window. Owing to the crystalline diamond low dielectric losses ( $\tan \delta = 2 \times 10^{-5}$ ) and high thermal conductivity ( $\sim 2,000 \text{ W/mK}$ ), simple edge water cooling of the window is possible. Disks of different thickness are used: 1.482 mm for the transmission of the 170 GHz wave and 2.592 mm for the transmission of both 170 GHz and 121.4 GHz, as shown in Figure 2.5.3-4.

<sup>1)</sup> M Thumm et al., "Status report on CVD-diamond window development, for high power ECRH" to appear in Fusion Eng. Des.

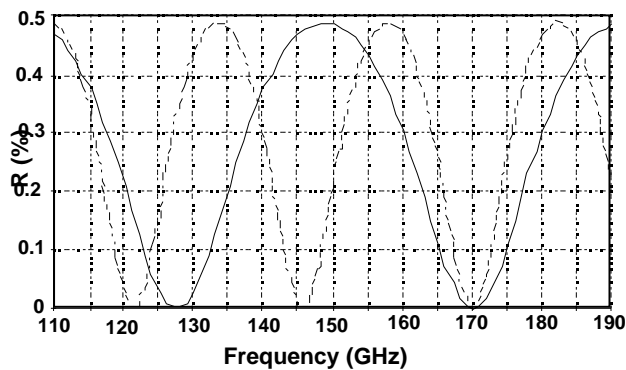


**Figure 2.5.3-4**  
**Power Reflectivity of Diamond Disk**  
 (solid line: reflectivity of a 1.482 mm disk;  
 dotted line: reflectivity of a 2.592 mm disk)

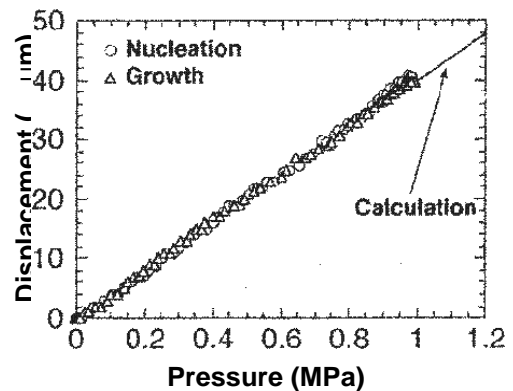


**Figure 2.5.3-5**  
**Pressure Test of a CVD Diamond**

The disk can withstand pressures up to 1 MPa, as demonstrated by pressure tests on a 70 mm disk, 2.25 mm thick (Figure 2.5.3.2-5)<sup>1</sup> This significantly exceeds the required 0.2 MPa value resulting from a LOCA in the vacuum vessel.

In the upper launcher<sup>2</sup> (Figure.2.5.3-3b) there are four steerable mirrors. A beam-mirror concept similar to that of the equatorial launcher is used, but now with eight beams, reflected in pairs by four mirrors through a vertical slot at the front shield. An additional fixed mirror is needed to reflect the beam through the slot, with an overall RF power loss of ~ 13 kW. An accurate focussing of the RF power on the  $m = 2$  and  $m = 3/2$  plasma flux rational surfaces is obtained

A complementary concept of remotely steerable launcher (Figure.2.5.3-6), allowing all movable components to be located outside the primary vacuum, has also been developed. Corrugated square cross-section waveguides and a fixed exit mirror are used. The steerable mirror is located outside the primary vacuum, at the input of the waveguide.

In a remotely-steered system, the square cross-section dimensions and the total waveguide length,  $L$ , must satisfy the relation  $L = 4a^2/\lambda$ , where  $\lambda$  is a wavelength and  $a$  is an internal width of the square waveguide. Here, the length of the waveguides is 6.5 m and  $a$  is ~ 50 mm. Fixed mirrors at the waveguide exit are used to reflect the RF beam  $-60^\circ \sim -70^\circ$  downward.

For steering angles  $< 10^\circ$  the beam optics are not degraded, as shown in Figure 2.5.3-7. It is also found that power transmission efficiency is not too sensitive to corrugation depth and wave guide alignment and steering can be obtained by a single axis rotation, if the steering angle is limited to  $\sim \pm 5^\circ$ . This allows the use of the same design for front and remote mirror assemblies. Both options are still under investigation.

<sup>1</sup> K.Takahashi et al., "Development and design of an ECRF launching system for ITER" to appear in Fusion Eng. Des.

<sup>2</sup> G. Bosia et al. "Design of ITER-FEAT RF H&CD system, Proc 21th IAEA Fus. Energy Conf., Paper ITERP14 (2000)

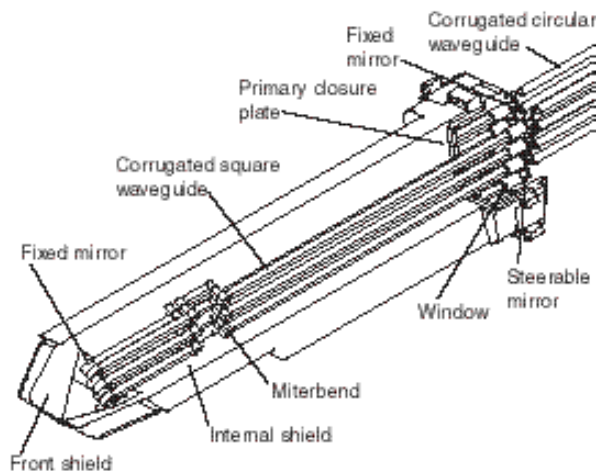


**Figure 2.5.3-6**  
**Upper Launcher (Remote Steering Type)**

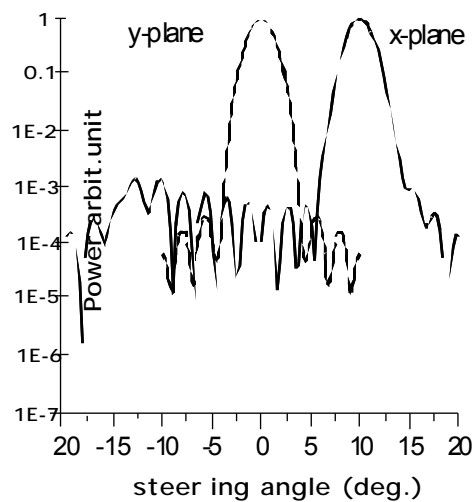


**Figure 2.5.3-7**  
**Steered RF Beam Profile**

### 2.5.3.3 Power Transmission Design

Transmission lines used by the EC system are commercial items and consist of:

- i. an RF conditioning unit;
- ii. straight sections of circular cross section corrugated wave guide;
- iii. a number of mitre-bends;
- iv. auxiliary equipment such as DC breaks, expansion segments, vacuum pumping sections, damping segments, isolation valves, sections including rupture discs and services (pumping, vacuum monitoring, water cooling, etc).

To reliably transmit the RF power, all sections of the transmission line are evacuated to  $10^{-3}$  Pa and water cooled. Pumping is provided at the RF conditioning unit. This converts the mm-wave power beam at the exit of the gyrotron to the waveguide  $HE_{11}$  mode, for long distance transmission. It consists of matching optics and a pair of polarizers.

The routing of the waveguides from the RF power sources to the tokamak is similar to the one shown in Figure 2.5.2-1. Transmission lines are grouped in the central area of the laydown, assembly and RF heating building and then directed to the tokamak. As the same RF sources are used to alternatively power the equatorial launcher and the three upper launchers, switching is provided at the exit of the RF heating area. The waveguides routed to the upper ports run along the tokamak hall south wall and penetrate the wall at different points. The total line length ranges from 70 m to 100 m depending on the gyrotron position. The overall power transmission efficiency, from gyrotron to injection point for both types of launchers, is about 80 %.

One torus window provides the primary vacuum confinement. An isolation valve (closing within 1 s) combined with a rupture disk, and exhausting in a volume connected to the detritiation system (VDS), provides the secondary confinement. When a high pressure accident happens in the vacuum vessel, the isolation valve closes. If the isolation valve shut-off fails, the rupture disc breaks and contaminated steam is conveyed by parallel ducts into the Vent Detritiation System.

#### 2.5.3.4 Power Source

High power mm waves are generated by a gyrotron drift-tube oscillator delivering an RF power of 1 MW in steady state. An efficiency of  $\sim 50\%$  is possible using a depressed-collector geometry. As the expected rf transmission losses are  $\sim 20\%$ , twenty four tubes and three 120 GHz gyrotrons are needed to inject 20 MW and 2 MW, respectively. An output window similar to the one described above is located at the gyrotron output.

Each power source (gyrotron unit) includes i) a tube and socket, ii) an oil tank, isolating the tube voltage supplies, iii) beam deflecting magnets (both normal and superconducting, and iv) electrical supplies for tube and magnets. The superconducting magnet (SCM) generates the magnetic field of 6.6 T at the cavity centre.

The gyrotron tube and associated power circuitry are protected by fast protection circuits, automatically ( $< 10 \mu\text{s}$ ) removing the DC body and cathode voltage in case of tube, line or load breakdown. After suitable vacuum conditions are recovered after the arc, the DC high voltages can be automatically re-applied. A regulated and variable DC high voltage power supply is required for the body and for the cathode of gyrotrons.

The gyrotron units located at the mezzanine level of the RF heating area in the laydown, assembly and RF heating building are arrayed in 7 groups (pods). A pod contains 4 tubes for the 170 GHz frequency and 3 tubes for 120 GHz. Each pod has common auxiliary supplies such as cooling water. Power supplies, series switches, and other auxiliary support equipment are located immediately below the gyrotrons on the lower level of the RF heating area. Each pod has separate control unit, interfacing to the power supply and capable of an independent operation.

### 2.5.4 **Ion Cyclotron H&CD System**

#### 2.5.4.1 General Design Features

The main heating scheme of the IC system is at the tritium second harmonic, in a 50-50% DT mixture at  $f = 53 \text{ MHz}$  and  $B_T = 5.3 \text{ T}$  with typical 50-50% power partition among the bulk ions and electrons. Addition of  $^3\text{He}$  ( $< 3\%$ ) minority [DT-( $^3\text{He}$ )] results in a significant increase of the fraction (up to 70%)<sup>1</sup> deposited on bulk ions. The alternative deuterium minority heating scheme is less efficient because it is in strong competition with absorption by Be and  $\alpha$ -particles.

The frequency window for on-axis current drive is at the peak of the electron absorption ( $f = 56 \text{ MHz}$ , with a central current drive efficiency of  $\sim 20 \text{ kA/MW}$ ). Ion minority current can be driven at the outboard  $q = 1$  for the control of the sawtooth period, at a frequency of 40 MHz.

The operating range  $f = 40 - 55 \text{ MHz}$  encompasses all the IC physics scenarios and allows operation at a 70% reduced toroidal field. An extension of the range (35 to 60 MHz), could be desirable for improved flexibility, and would be possible at somewhat reduced performance.

---

<sup>1</sup> P. Bergeaud et al., Nuclear Fusion 40 (2000) 35

**Table 2.5.4.1-1 Ion Cyclotron Resonances**

Resonance	MHz	Comments
$2 \tau = {}^3\text{He}$	53	Second harmonic + minority heating
D	40	Minority heating. Strong competition of Be and $\alpha$ -particles
FWCD	56	On axis current drive
${}^3\text{He}$	45	Minority ion current drive at sawtooth inversion radius (outboard)

The IC system is designed to operate, at the nominal power density:

- at a moderate electric field at the plasma interface and in-vacuum ( $E_{\text{max}} < 2 \text{ kV/mm}$ );
- at a power transfer efficiency essentially constant over the frequency range;
- with a high tolerance to load variations not to require dynamic matching control in ELMy plasmas.

The system performance is computed as a function of plasma loading  $R' = (2P/I^2)^{1/2} (\text{ } / \text{m})$ , where  $I$  is the maximum strap current and  $P$  is the radiated power per unit length, by modelling the array/tuning system as a network of lossy and coupled transmission lines. The nominal  $R'$  value used in the computations (perfect match at  $4 \text{ } / \text{m}$ ) is typical for ITER operation at 53 MHz, phasing, at a gap of 120 mm from the separatrix. The main results are summarised in Table 2.5.4.2-1.

**Table 2.5.4.2-1 Summary of Array Parameters (at  $R' = 4 \text{ } / \text{m}$  and  $f = 55 \text{ MHz}$ )**

Parameter	Value	Parameter	Value
Strap length (m)	0.3	MTL Voltage (kV)	12.25
Characteristic impedance ( )	$\sim 35.0$	Max voltage in tuner (kV)	32.1 & 40.0
Feeder length(m)	0.3	Max voltage in choke(kV)	5.4
Matched reactances (1&2) ( )	-38.3 & -49.7	Max E-field in tuner (V/mm)	1.99 & 2.45
RDL Input impedance ( )	6	Max E-field in choke (V/mm)	0.28
Input power (MW)	2.5	Max E-field in strap (V/mm)	1.3
Tuners @ choke char. imp.( )	10	Max E-field in VTL (V/mm)	0.53
Input voltage (kV)	5.5	Power transfer efficiency (%)	$\sim 95$
Max. strap voltage (kV)	27	Variation of PE with freq. (%)	$\sim 5$
Max. strap current (kA)	1.30		

All requirements are met. In particular, the voltage standing wave ratio at the input of the resonant double loop (RDL) remains below 1.5 (Figure 2.5.4-1) for any loading  $R' > 2.5 \text{ } / \text{m}$ . This implies that load variations such as those caused by ELMs can be accepted without the need of real-time re-tuning.

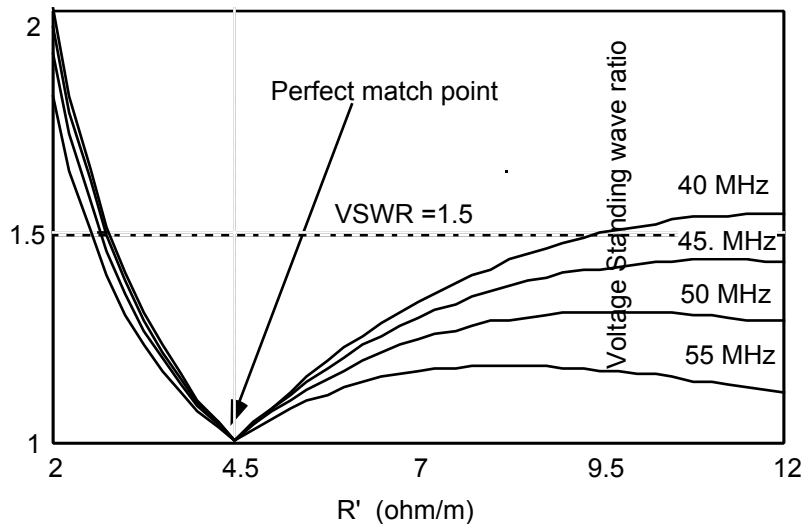


**Figure 2.5.4-1** Input VSWR as Function of  $R'$  and Frequency

### 2.5.4.2 Launcher Design

The IC launcher is an array of 4x2 elements fed by eight coaxial transmission lines each carrying a nominal RF power of 2.5 MW (Figure 2.5.4-2).

The electric scheme of the IC antenna is a variation of the resonant double loop (RDL) concept. The RDL consists of a pair of straps with capacitive tuners in series, located at the input (Figure 2.5.4-3a). The straps are short, with one end connected to ground (Figure 2.5.4-3b). This arrangement makes them self supporting and able to operate at low voltage

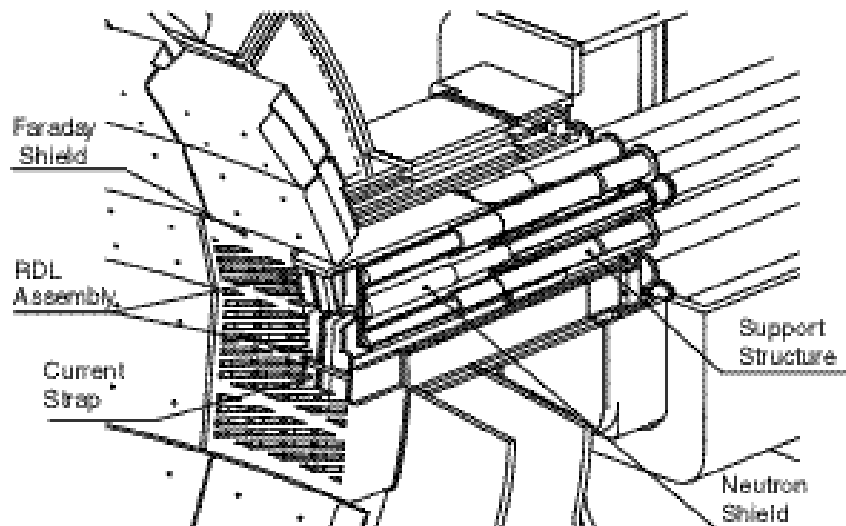


**Figure 2.5.4-2** View of the IC Array Seen From the Plasma

The tuners are sections of coaxial transmission lines, the electrical length of which is varied by sliding a short circuit to the opposite end. The adjustable lines and their actuators are located in tubular assemblies (Figure 2.5.4-3b), individually removable for maintenance.

The tuners are inserted in cylindrical cavities of the neutron shield, forming outer coaxial structures (chokes) whose electrical length is set at  $\lambda/4$  by sliding short circuits similar to

those of the tuners. The chokes decouple the inputs of the tuners and have all the same length. They are also housed in the removable sections of the tuners.

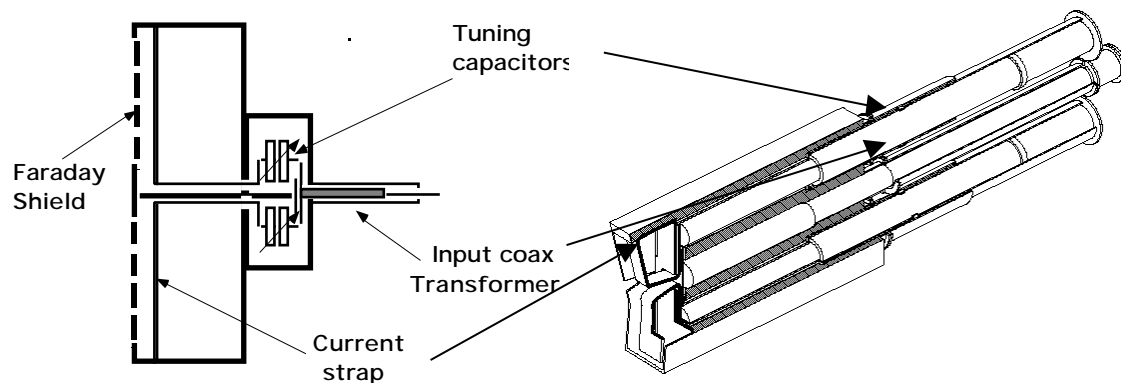


**Figure 2.5.4-3 a) Electrical Scheme of RDL Antenna; b) Mechanical Layout**

The two-strap/tuner assemblies are connected in parallel to the vacuum transmission line and matched at a low input resistance ( $6 \Omega$ ). It can be shown that this scheme features a large tolerance to load variations. A wide-band impedance transformer, located in the coaxial feeder, transforms the input impedance to the VTL characteristic impedance ( $30 \Omega$ ).

The IC array features a modular construction. A box-like, Be-plated, Faraday shield in Cu-Cr-Zr alloy, is the plasma-facing component, with elements tilted  $16^\circ$ , to be approximately aligned with the local magnetic field. Eight RDL structures, with coaxial tuners inserted in the neutron shield are fed by eight coaxial feeders, (Figure 2.5.4-4).

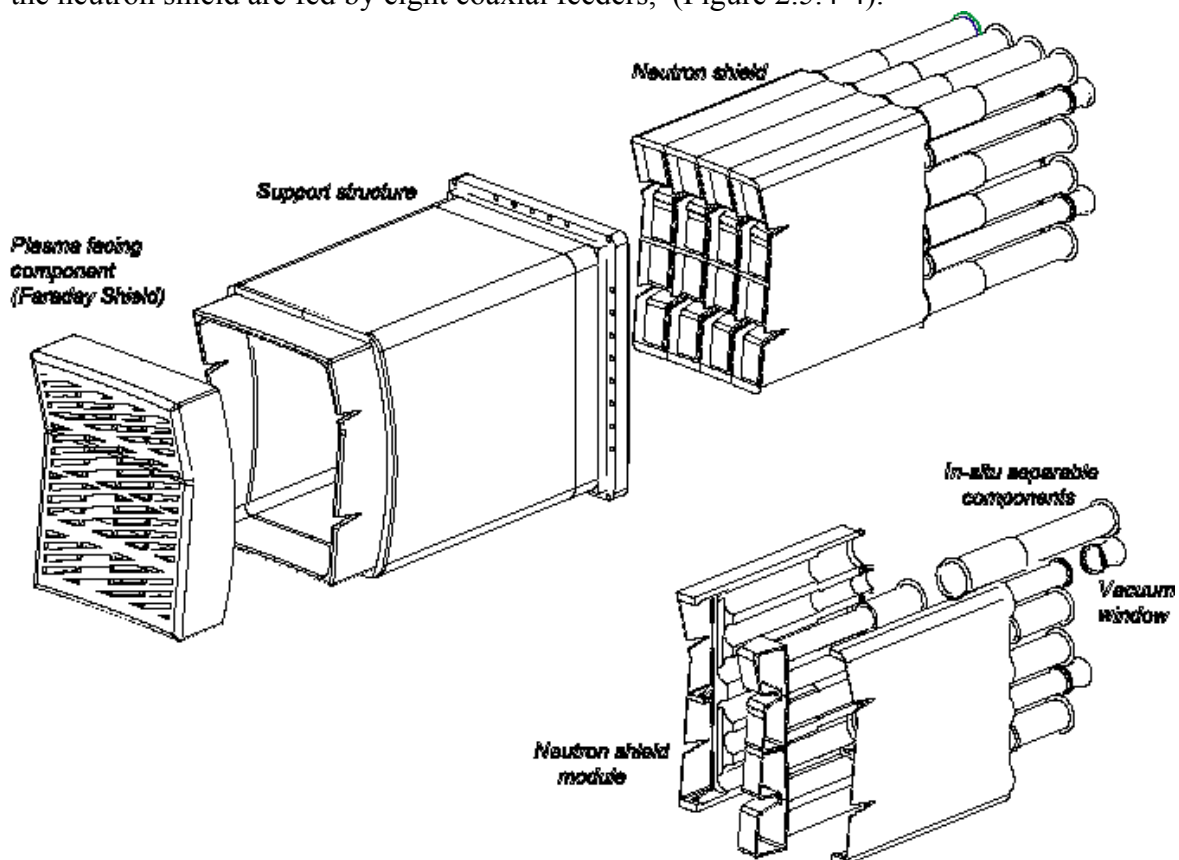


**Figure 2.5.4-4 Exploded View of IC Launcher Showing Main Mechanical Components and Ways for Disassembly**

These components are mechanically assembled with and supported by the outer mechanical structure (in 316L(N)-IG SS), also enclosing coolant manifolds for the front-end components. The closure plate supports the eight IC vacuum transmission line ceramic (BeO) feed-throughs, contributing to the vacuum and tritium containment. The windows are also accessible from behind and can be easily maintained

#### 2.5.4.3 Power Transmission Design

The coaxial transmission lines used by the IC system are commercial items. The main transmission line is a rigid coaxial of 280 mm OD, having a characteristic impedance of 30  $\Omega$ . The inner conductor is radiation-cooled and operates at  $T_{in} < 110^\circ\text{C}$ . The outer conductor is water-cooled and operates at  $T_{out} \sim 45^\circ\text{C}$ . The two conductors are coated with high emissivity material to enhance radiative thermal exchanges.

The voltage stand-off of the main transmission line is 80 kV, well in excess of the expected maximum RF voltage ( $< 15$  kV). This large margin should provide low maintenance and a high reliability to this component.

#### 2.5.4.4 RF Power Sources

The IC power sources are commercial multi-stage amplifiers equipped with tetrode tubes. The power source delivers 2.5 MW CW in a mismatched load with VSWR  $< 1.5$ . A detailed study has shown that this source can be constructed either using two existing commercial tetrodes combined in the end stages, or by a single-tube end-stage, with an upgraded anode power dissipation.

### 2.5.5 **Lower Hybrid System**

#### 2.5.5.1 General Design Features

The lower hybrid H&CD system is specialised for off-axis current drive and current profile control. It is designed to deliver a total power of 20 MW at 5 GHz to the ITER plasma.

Typically, the system can drive a plasma current at a flux surface  $y$  such as  $n_e(y)T_e(y) \sim 10\text{-}15 \times 10^{20}$  keV  $\text{m}^{-3}$ , with a typical current drive efficiency between 2 and  $3 \times 10^{20}$   $\text{m}^{-3}$  MA/MW, in any scenario and/or discharge phase. In ITER, this is approximately equivalent to a driven current of  $\sim 1.5$  MA in the region  $0.5 < r/a < 0.7$ .

An efficient coupling of LH to the plasma requires the presence of a sufficient plasma density between the launcher and the separatrix ( $4 \times 10^{17}$   $\text{m}^{-3}$   $n_e$   $10 \times 10^{17}$   $\text{m}^{-3}$ ).

The system is designed to operate at:

- a waveguide maximum electric field of 3.2 kV/mm (or a power density of 33 MW/m<sup>2</sup>) at full power;
- a wave number  $1.8 < n_{//} < 2.2$  modified by electronically varying the array phasing;
- a maximum load reflection coefficient of 5%, measured at the antenna input.

### 2.5.5.2 Launcher Design

The LH launcher is shown in Figure 2.5.5-1. The plasma-facing component is a phased array, made of four modules (2x2) of passive-active multi-junction (PAM) stacks. Each PAM module is composed of 24 active and 25 passive, rectangular cross section wave guides, progressively phased in quadrature, so as to synthesize a travelling slow wave propagating in the toroidal direction. The phase shift is obtained by inserting phase shifters of multiples of  $\pi/2$  in adjacent groups of waveguides. Details on the mechanical dimensions of the PAM stack are listed in Table 2.5.5-1.

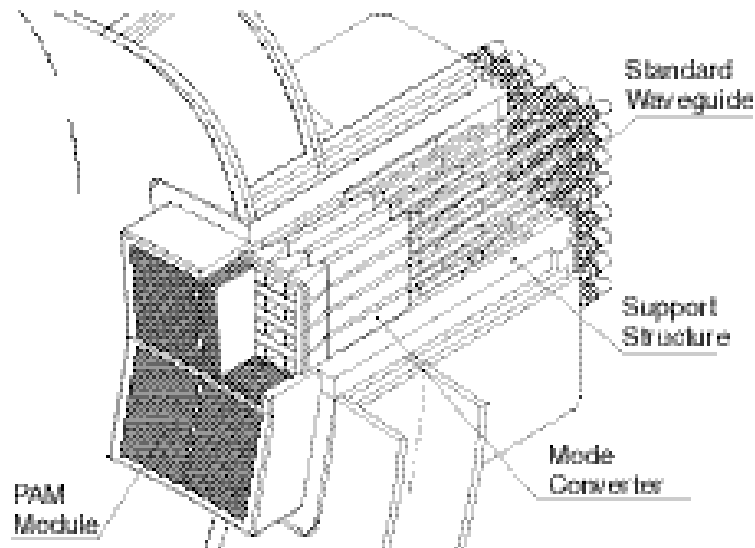


**Figure 2.5.5-1 LH Launcher**

**Table 2.5.5-1 Mechanical Dimensions of Multi-junction Stack**

Parameter	Value
Number of active wave-guides	24
Number of passive wave-guides	25
Cross section of active wave-guide (mm <sup>2</sup> )	9.25 x 171
Mechanical length (mm)	900
Fundamental transmission mode	TE <sub>30</sub>
Mechanical length (mm)	925 to 1050
Wall thickness (mm)	13.25
Phasing among active wave-guides	3 $\pi$ / 2
Phase shifter dimensions (mm)	14 x 750
Typical n// value	1.9-2.1
Max electric field in nominal power (22%) plasma reflection (kV/cm)	3.2

The PAM assembly is constructed in precipitation-hardened copper alloy (CuCrZr) or in dispersion-strengthened copper alloy (Glidcop Al25) and covered by a Be protection plate 18 mm thick. Cooling channels are provided in the thickness of the passive wave guide wall, by twin cooling channels lined with thin 316LN SS tubing, and supplied by a manifold housed in the supporting frame.

Forty-eight TE<sub>10</sub>/TE<sub>30</sub> mode converters form a 2x2 matrix, held in position by a 316LN SS frame, which also provides the attachment of the launcher to the support structure. The mode converters are cooled by means of channels bored in their top and bottom SS walls. The same cooling circuit feeds all cooling channels in the module. The mode converters are fabricated of 316 LN SS, Cu-plated on the inside surfaces.

Forty-eight double-disk ceramic windows (12 per module) are located at the end of each converter, outside the primary closure plate. BeO (99% purity) is used as dielectric material. The windows have an insertion loss of 0.1%, a voltage standing wave ratio VSWR ~ 1.5, and a working frequency of 5 GHz ± 1 MHz. The ceramic disks can withstand 0.2 MPa dry air pressure on one side. The coolant is routed to the components of the four PAM modules from a common manifold located in the support structure, and connected to the primary heat transfer system.

### 2.5.5.3 Power Transmission Design

The main transmission line (MTL) is in four sections.

i) A vacuum section (Figure 2.5.5-2) which runs between vacuum vessel and cryostat closure plates. The VTLs are commercial rigid rectangular waveguide sections (type WR229), connected in pairs to 24 3-dB hybrid junctions. At the cryostat exit, twenty-four standard vacuum windows or gas barriers are used for secondary vacuum containment.

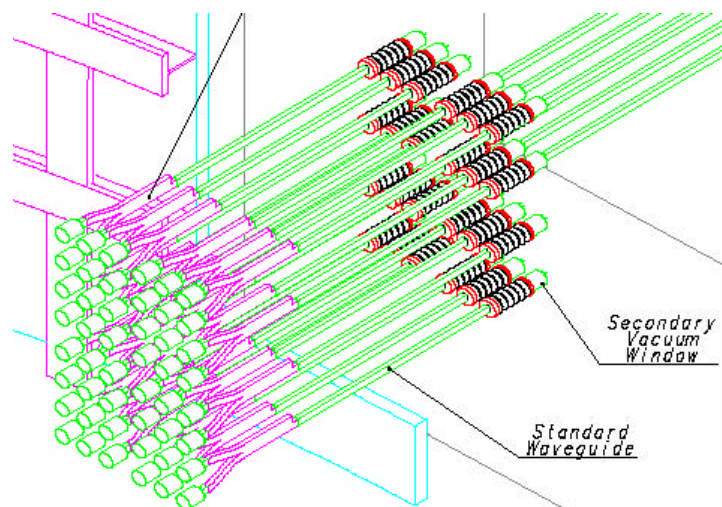


**Figure 2.5.5-2 Vacuum Section of MTL**

ii) A pressurised splitting network section (SN), running from the cryostat wall and the circular transmission line. Each circular wave-guide feeds 4 standard vacuum transmission lines through its SN.

iii) A pressurised circular transmission line section (CTL), running from the splitting network to the klystron cabinet (Figure 2.5.5-3). The total CTL length is approx. 80 m with six 90° bends. The circular transmission line is made of sections of commercial, rigid circular cross-section waveguide and elbows, filled with pressurised air. The main propagating mode

is  $TE_{01}$ . Mode filters are inserted along the line, to avoid propagation of high order modes (see Table 2.5.5-2).

iv) A pressurised recombining network (RN) section (symmetric with the SN), located in the klystron cabinet, running from the CTL to each individual power klystron. Each MTL is fed by 4 klystrons through the RN.

Four klystron generators are connected to the same CTL through the RN, which includes an RF switch and a 1 MW test load.

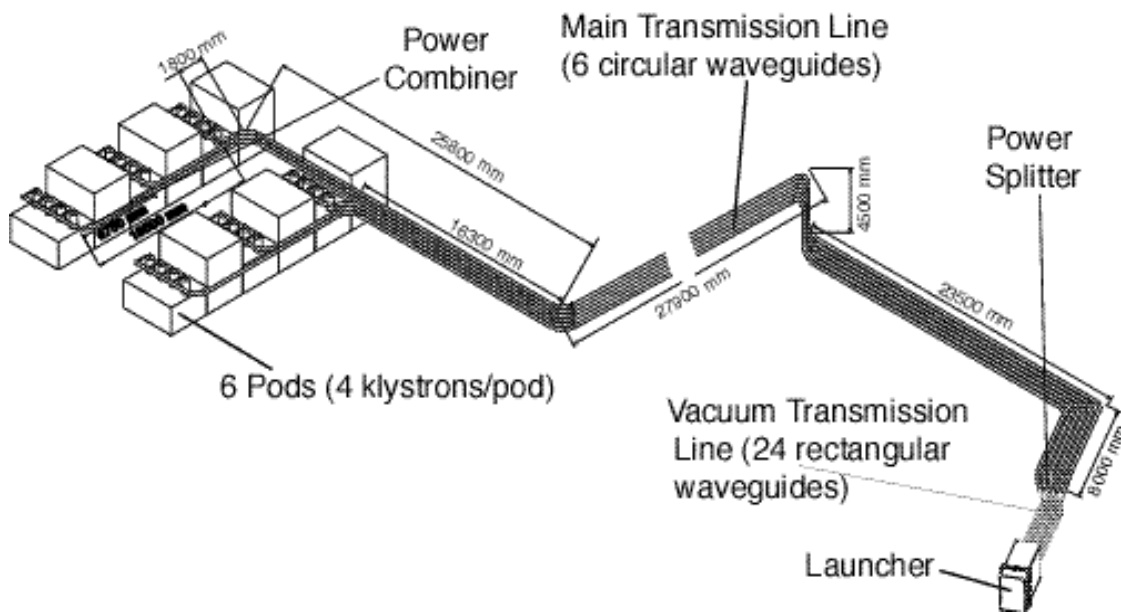


**Figure 2.5.5-3 Pressurised Section of MTL and Power Sources Layout**

**Table 2.5.5-2 Main Transmission Line Parameters**

Design	Feature
Wave guide	standard C10: 107.57 mm radius
Flange	remote handling and standard C 10 types
Material	OFHC, 3 mm thick
Attenuation $TE_{01}$ @ 5 GHz (dB/m)	$4.2 \times 10^{-4}$
RF power rating	4 MW
Electric field for nominal operation at VSWR = 1	822 V/m
VSWR	< 1.4
Admissible operating pressure	4 bar absolute
Sealing material	Silicon rubber
Insertion loss for a 90° bend	< 0.3 %
Insertion loss for mode filter or bellows	< 0.5 %
Bellows span	+/- 10 mm

#### 2.5.5.4 RF Power Sources

The LH RF power system consists of 24 RF power sources, each consisting of one power klystron amplifier (see Table 2.5.5-3) and of auxiliaries (focusing block with superconducting magnet and regulated supply, shielding, filament power supplies, and oil tank). The amplifier is driven by a solid state driver amplifier (10 W).

Phase and amplitude of the output wave of all klystrons are electronically controlled using a single reference. The klystrons are connected in groups of four to the HVDC power supply unit and common protection circuits are installed close by so as to minimize stray capacitance in the connections.

**Table 2.5.5-3 Main Features of the Klystron Amplifier**

Nominal power	1 MW (VSWR < 1.4:1 any phase), CW
Duty cycle	CW or 1000s every 20 mn
Frequency	5 GHz
Bandwidth	1 MHz
Efficiency	> 60 %
Gain	53 dB
Amplitude accuracy	1%
Phase accuracy	$\pm 2^\circ$